GEOLOGY | THE GEOLOGICAL SOCIETY OF AMERICA®

https://doi.org/10.1130/G49458.1

Manuscript received 4 April 2021
Revised manuscript received 4 July 2021
Manuscript accepted 12 August 2021

Published online 20 October 2021

Volcanic origin of the mercury anomalies at the Cretaceous-Paleogene transition of Bidart, France

Eric Font[1,2], Jiubin Chen[3], Marcel Regelous[4], Anette Regelous[4] and Thierry Adatte[5]

[1]Departamento de Ciências da Terra, Faculdade de Ciências e Tecnologia, Universidade de Coimbra, 3000-272 Coimbra, Portugal
[2]Instituto Dom Luís (IDL), Faculdade de Ciências, Universidade de Lisboa, 1749-026 Lisbon, Portugal
[3]School of Earth System Science, Institute of Surface-Earth System Science, Tianjin University, Tianjin 300072, China
[4]GeoZentrum Nordbayern, Universität Erlangen-Nürnberg, Schloßgarten 5, 91054 Erlangen, Germany
[5]Institute of Earth Sciences (ISTE), Lausanne University, Geopolis, CH-1015 Lausanne, Switzerland

ABSTRACT

The timing and mechanisms of the climatic and environmental perturbations induced by the emplacement of the Deccan Traps large igneous province (India) and their contribution to the Cretaceous-Paleogene (K-Pg) mass extinction are still debated. In many marine sediment archives, mercury (Hg) enrichments straddling the K-Pg boundary have been interpreted as the signature of Deccan Traps volcanism, but Hg may also have been derived from the Chicxulub (Mexico) impact. We investigated the Hg isotope composition, as well as the behavior of iridium (Ir) and other trace elements, in K-Pg sediments from the Bidart section in southwest France. Above the K-Pg boundary, Ir content gradually decreases to background values in the Danian carbonates, which is interpreted to indicate the erosion and redistribution of Ir-rich fallouts. No significant enrichment in Ir and W, or Zn and Cu, is observed just below the K-Pg boundary, excluding the hypothesis of downward remobilization of Hg from the boundary clay layer. Positive Δ^{199}Hg and slightly negative values in the upper Maastrichtian and lower part of the early Danian are consistent with the signature of sediments supplied by atmospheric Hg^{2+} deposition and volcanic emissions. Up section, large shifts to strongly negative mass-dependent fractionation values (δ^{202}Hg) result from the remobilization of Hg formerly sourced by the impactor or by a mixture of different sources including biomass burning, volcanic eruption, and asteroid impact, requiring further investigation. Our results provide additional support for the interpretation that the largest eruptions of the Deccan Traps began just before, and encompassed, the K-Pg boundary and therefore may have contributed to the K-Pg mass extinction.

INTRODUCTION

The cause of the Cretaceous-Paleogene (K-Pg) mass extinction is a long-standing debate and it is certainly the most disputed of the "Big Five" mass extinctions that punctuated the evolution of life on Earth. The compelling evidence that an asteroid impact was the primary cause of the K-Pg mass extinction (Alvarez et al., 1980; Schulte et al., 2010) has been opposed by the idea that the Deccan Traps (in India) drove the extinction instead (Courtillot et al., 1986; Keller et al., 2020). Recent high-precision radiometric ages indicate that the emplacement of the largest lava formations of the Deccan Traps began shortly after (Sprain et al., 2019) or before (Schoene et al., 2019) the Chicxulub (Mexico) impact. The sedimentary record of Deccan Traps eruptions is more challenging to discern and relies mostly on the correlation of the age of the Deccan lava flows with mercury (Hg) concentrations recorded in marine sediments, which are taken as a proxy for increased volcanic input (Sial et al., 2013, 2014, 2016; Font et al., 2016; Keller et al., 2018, 2020; Meyer et al., 2019). At Bidart (southwestern France), one of the best preserved K-Pg transitions in Europe, Hg anomalies are observed in the last meter of the Maastrichtian section and continue in the lower part of the early Danian (Font et al., 2016). The Hg anomalies are associated with an interval of low magnetic susceptibility (Fig. 1) located just below the K-Pg boundary, which also contains akaganeite, constituting another key piece of evidence for Deccan Traps volcanism in this sedimentary interval (see the review in Font and Bond [2021]). However, the high Hg contents have also been attributed to postdepositional Hg enrichment by downward remobilization of Hg deposited at the K-Pg boundary by the Chicxulub impact, or contained in anoxic sediments deposited immediately following the impact (Smit et al., 2016). Understanding the origin of these Hg anomalies is essential to resolving the timing of Deccan Trap eruptions relative to the K-Pg extinction and the Chicxulub impact. We examined the Hg isotope record at Bidart, and our results show that enhanced volcanism initiated prior to, and extended across, the K-Pg extinction boundary.

MATERIALS AND METHODS

The Bidart section crops out along the Erreteguia beach 2 km north of the city of Bidart and can be accessed by highway R.N.10 (43°26′N, 1°35′W). It consists of hemipelagic to pelagic sediments deposited at upper-middle bathyal depths in the Basque-Cantabric Basin in southwestern France. The Maastrichtian interval is dominated by marls and calcareous marls, whereas Danian sediments are composed of pink and white biogenic limestone beds. The K-Pg boundary is identified in the field by a distinctive thin ~1-cm-thick gray clay layer containing the globally recognized Ir anomaly (Bonté et al., 1984). Font et al. (2016) presented Hg concentration data from 37 samples (green points in Fig. 1).

We complemented our previous work by analyzing the bulk and isotopic Hg composition and total organic carbon (TOC), Ir, W, Cu, and Zn contents of 44 additional samples located in the upper Maastrichtian and Danian intervals of the Bidart section (Table S1 in Supplemental

CITATION: Font, E., et al., 2021, Volcanic origin of the mercury anomalies at the Cretaceous-Paleogene transition of Bidart, France: Geology, v. XX, p. , https://doi.org/10.1130/G49458.1

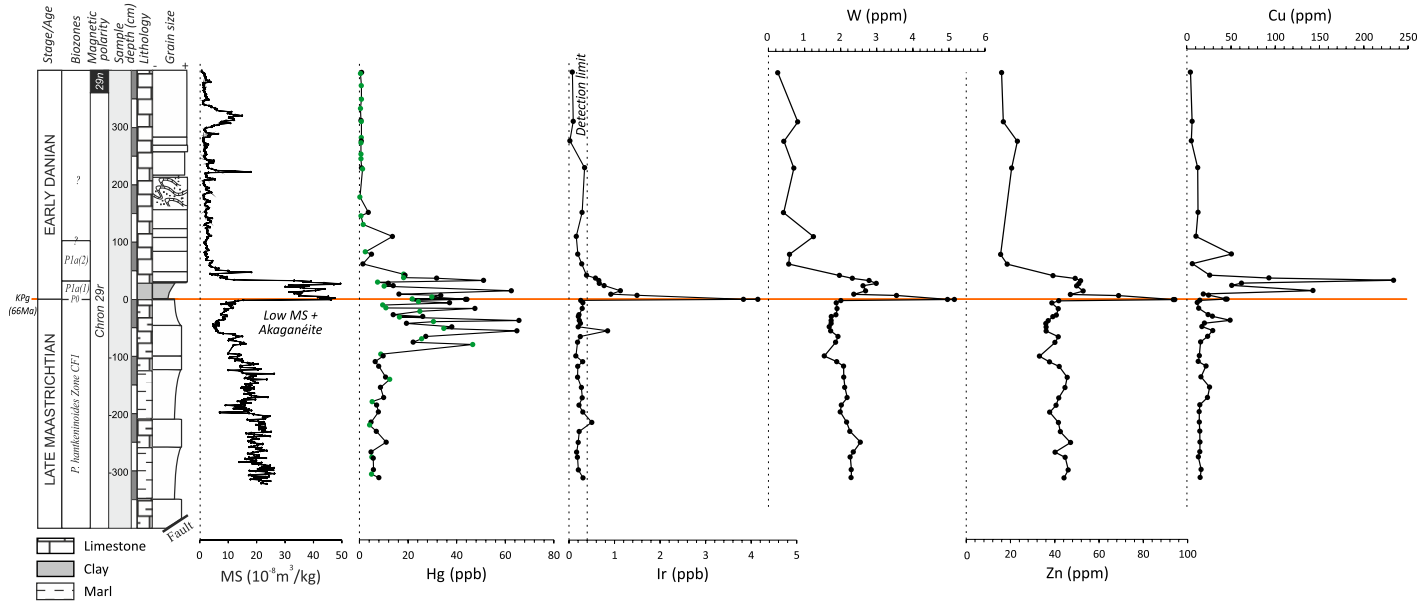

Figure 1. Magnetic susceptibility (MS) of Bidart (southwestern France) sediments (Font et al., 2011), and Hg, Ir, W, Zn, and Cu concentrations (this study). Green circles in the Hg (ppb) curve correspond to samples previously reported by Font et al. (2016); black circles correspond to this study. KPg—Cretaceous-Paleogene boundary; *P. hantkeninoides—Plummerita hantkeninoides*; Pla(l), Pla(2)—planktic foraminiferal zones.

Material[1]). Hg content was measured by atomic absorption spectrometry using a DMA-80 direct Hg analyzer (Milestone Srl, Italy) from MWS/MLS GmbH (Germany) at the GeoZentrum Nordbayern, Erlangen, Germany. Ir, W, Cu, and Zn concentrations were determined by quadrupole inductively coupled plasma–mass spectrometry (ICP-MS) at the GeoZentrum Nordbayern. Mercury isotope ratios were determined by multicollector (MC) ICP-MS (Nu-Plasma, Nu Instruments) at the Institute of Surface-Earth System Science of Tianjin University, China, following a method similar to Huang et al. (2015). Detailed analytical methods are available in the Supplemental Material.

RESULTS

Our new data show that Ir contents are generally below detection limit (0.40 ppb) in Maastrichtian samples and shift abruptly to values of 3.83 and 4.15 ppb at the K-Pg boundary (Fig. 1). These values are consistent with the concentration of 6 ppb previously found by Bonté et al. (1984). Ir concentrations gradually decrease in the next 50 cm above the K-Pg boundary, down to values lower than 0.60 ppb in the upper part of the early Danian carbonates. Other more-mobile elements like Zn, W, and Cu behave similarly to Ir and show no enrichment relative to background values below the K-Pg boundary.

For comparison, Figure 2 illustrates previously reported Hg content (Font et al., 2016) together with the new Hg measurements obtained here. Hg enrichments start in the upper Maastrichtian interval, ~75 cm below the K-Pg boundary, and end in the lower part of the early Danian, ~40 cm above the K-Pg boundary (Table S1). Two samples from the clay boundary yielded values of 43.7 and 44.3 ppb (21.8 ppb in the clay layer analyzed by Font et al. [2016]), while maximum values of 62.5 and 65.7 ppb were observed in samples located just above and below the boundary, respectively (Table S1). Because organic matter content is very low (TOC <0.15%), normalization of Hg by TOC is not needed.

In the basal Maastrichtian marls, Δ^{199}Hg shows positive values between 0.06‰ and 0.24‰ ($2\sigma < 0.10$‰). In the 50 cm above the K-Pg boundary, Δ^{199}Hg shows slightly more positive values of 0.16‰–0.46‰ ($2\sigma < 0.05$‰). The δ^{202}Hg values are −2.17‰ to −0.12‰ in the Maastrichtian and lower part of the early Danian (biozones P0–P1a[1] in Fig. 2), whereas upper Danian carbonates show more negative δ^{202}Hg values down to −4.87‰ ($2\sigma < 0.31$‰).

DISCUSSION

Studies of modern systems have shown that Hg, as well as other metals like Cu and Zn, is quite immobile and exhibits stable sediment profiles once deposited, except in some marine settings with extremely low sedimentation and mixing rates and organic matter–poor lakes (Gobeil et al., 1999; Feyte et al., 2012; Percival and Outridge, 2013). At Bidart, Hg could have been deposited by the impact or enriched/scavenged by anoxia on the seafloor and subsequently penetrated into uppermost 10–50 cm of the Maastrichtian interval (Smit et al., 2016). Ir has also been considered to be an element of relatively low mobility, but it can be remobilized by postdepositional processes and changes in sedimentary redox conditions (see the review in Evans and Chai [1997]; Martin-Peinado and Rodriguez-Tovar, 2010). In well-preserved K-Pg boundary records, Ir and other platinum group elements exhibit peak concentrations within the clay boundary layer, but anomalies are also described both above and below the boundary. High Ir concentrations above the clay boundary, as observed at Bidart, may result from erosion and redistribution of Ir-rich fallout deposited onto continental surfaces after the impact (e.g., Preisinger et al., 1986). Extension of the Ir anomaly below the clay boundary is better explained by physical reworking by bioturbation (Pospichal et al., 1990; Zhou et al., 1991), or remobilization during diagenetic alteration or the existence of a reducing environment at the time of deposition (e.g., Colodner et al., 1992). At Bidart, the absence of any Ir anomaly immediately below the K-Pg clay boundary demonstrates no downward Ir remobilization. W, Zn, and Cu show similar behavior to Ir, with low concentrations in the Hg-enriched sediments below the impact layer (Fig. 1). We conclude then that the Hg enrichment below the K-Pg boundary at Bidart did not result from the impactor, or remobilization of Hg from the boundary clay, and thus requires an alternative explanation.

Hg is derived from sources such as volcanoes, natural combustion of coal, biomass burning, and asteroid impacts. Thus, there could be a mixed source of Hg. Asteroid impactors can

[1]Supplemental Material. Detailed analytical methods, Table S1 (Hg concentration, total organic carbon, and Ir concentration of the Bidart samples), Table S2 (Hg isotope composition of the Bidart samples), and methods. Please visit https://doi.org/10.1130/GEOL.S.16725460 to access the supplemental material, and contact editing@geosociety.org with any questions.

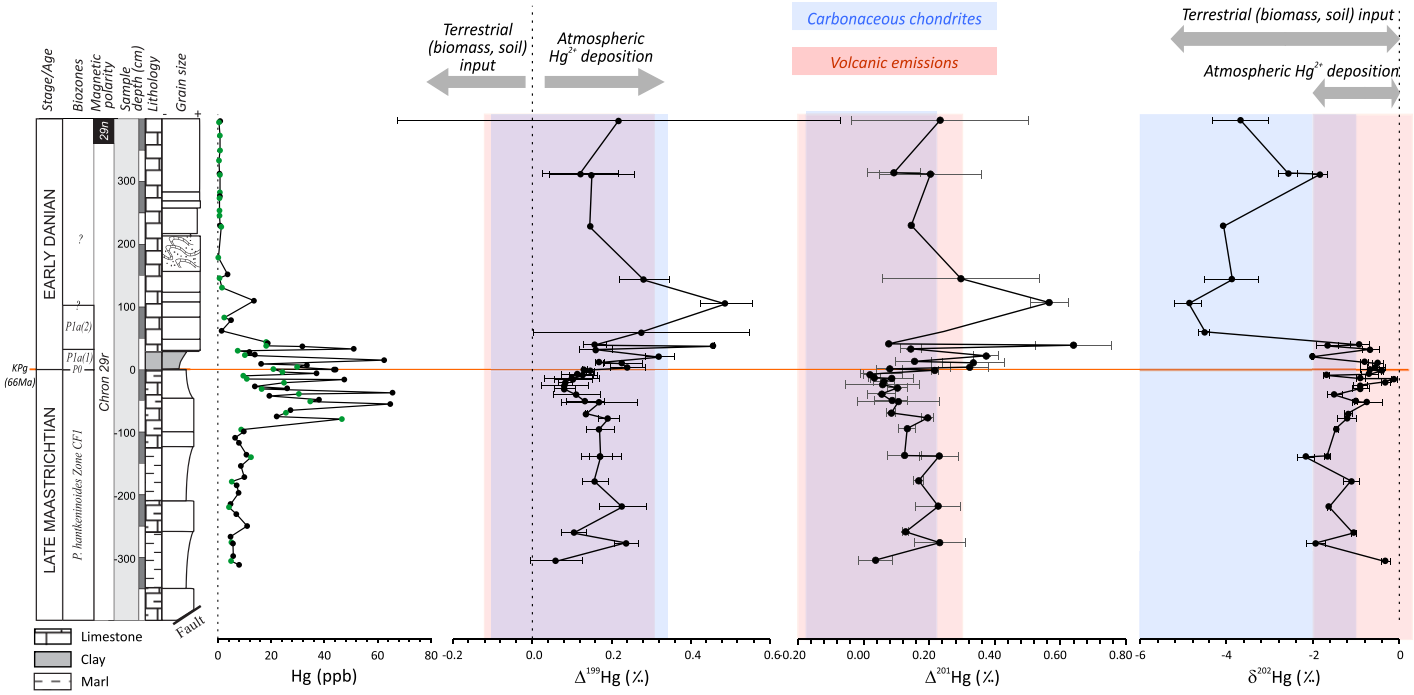

Figure 2. Bulk Hg content and mass-independent (Δ^{199}Hg) and mass-dependent (δ^{202}Hg) fractionation of Hg isotopes at Bidart (southwestern France). Δ^{199}Hg and δ^{202}Hg values are given with 2σ error. Typical values of volcanic emissions (gas and particulate) and carbonaceous meteorites are from Zambardi et al. (2009) and Meier et al. (2016), respectively. *P. hantkeninoides—Plummerita hantkeninoides*; Pla(l), Pla(2)—planktic foraminiferal zones.

contain significant amounts of Hg, albeit with a large variability within the same meteorite and depending on the type of meteoritic material. Lauretta et al. (2001) reported bulk Hg abundance of ~294 ppb and ~30 ppb in the Murchison and Allende meteorite carbonaceous chondrites, respectively. Meier et al. (2016) measured Hg abundances between 12 ± 2 ppb (meteorite Dhofar 1432) and 13,600 ± 5600 ppb (meteorite Orgueil) for carbonaceous chondrites. The Hg concentrations of Meier et al.'s sample of Murchison yielded concentrations of ~2500 ppb; i.e., one order of magnitude higher than that reported by Lauretta et al. (2001). Meier et al. (2016) showed that the large variability of Hg content found in different samples from the same meteorite is not due to terrestrial Hg contamination, but is rather controlled by the strongly heterogeneous distribution of the Hg-carrying phases at the centimeter scale. Despite the large differences in bulk Hg abundances in individual meteorites, it is possible that part of the Hg observed at, and/or immediately above, the K-Pg boundary came from the Chicxulub impactor. In many K-Pg sections, including Bottacione in Italy, Elles in Tunisia, and Stevns Klint in Denmark, the highest Hg contents and Hg/TOC ratios are observed at the clay boundary (Sial et al., 2013; Keller et al., 2020). At Bidart, Hg anomalies start 75 cm below the K-Pg boundary, with the highest values in the upper Maastrichtian interval, and anomalies continue into the lower part of the early Danian interval (Font et al., 2016; this study; Fig. 1). There is no distinct Hg enrichment at the K-Pg boundary clay.

Mercury has a complex and active biogeochemical cycle, including redox, biological, and phase transformations, which may induce mass-dependent fractionation (MDF) and/or mass-independent fractionation (MIF) of Hg isotopes, providing useful information about the sources and the mechanisms responsible for Hg enrichments (Bergquist and Blum, 2009; Blum et al., 2014; Grasby et al., 2019). Although the exact carbonaceous chondrite type of the Chicxulub impactor is not known, nor how representative the MDFs measured in individual meteorites really are for asteroid-sized bodies (Meier et al., 2016), Hg isotopes could help to distinguish the volcanic and meteoritic contributions to the Hg anomalies found at Bidart. For instance, Hg emitted by volcanoes generally have no MIF (noted as Δ^{199}Hg), whereas carbonaceous chondrites have a MIF signature (Δ^{199}Hg excess). Both have MDF (noted as δ^{202}Hg) signatures, but whereas volcanic gas and particulates have MDF of −1.74‰ ± 0.36‰ for plume gaseous elemental $Hg^0_{(g)}$ and −0.11‰ ± 0.18‰ for plume particulate $Hg^{II}_{(p)}$ (Zambardi et al., 2009), carbonaceous chondritic meteorites possess much more negative values of −7‰ to −1‰ (Meier et al., 2016; Moynier et al., 2020). Once emitted into the atmosphere, $Hg^0_{(g)}$ is readily oxidized into Hg^{2+} species or directly absorbed by vegetation and soils. Aqueous photoreduction of Hg^{2+} in cloud droplets and surface waters induces large MIF, leading to positive Δ^{199}Hg values in the residual aqueous Hg^{2+} pool (Bergquist and Blum, 2007). Therefore, atmospheric Hg^{2+} and sediments dominated by atmospheric Hg^{2+} deposition generally have δ^{202}Hg values close to 0 and slightly negative (~−2‰ to 0‰) or positive Δ^{199}Hg values. In contrast, in terrestrial reservoirs, additional MIF and MDF occur during the sequestration of $Hg^{(0)}_{(g)}$ by plant and soils, leading to negative Δ^{199}Hg values and much more negative δ^{202}Hg values than atmospheric $Hg^{(0)}_{(g)}$. The sediments carrying the Hg anomalies at Bidart have positive Δ^{199}Hg (0.08‰ ± 0.06‰ to 0.46‰ ± 0.00‰) and slightly negative δ^{202}Hg (−2.01‰ ± 0.00‰ to −0.12‰ ± 0.07‰) values. These values are consistent with a volcanic origin for the Hg anomalies (Fig. 2), where positive Δ^{199}Hg values reflect photoreduction of Hg^{2+} during atmospheric transport (Grasby et al., 2019). The δ^{202}Hg values of the Bidart sediments are also consistent with volcanic gases and particulate values like those of Vulcano (Italy) (Zambardi et al., 2009). Based on these isotope data, we argue that the Hg anomalies initiating prior to, and extending across, the K-Pg boundary are related to greatly enhanced volcanism at that time, with the most reasonable source being the Deccan Traps, which are dated to have been erupting contemporaneously (Schoene et al., 2019).

Hg isotope compositions of meteorites are less well documented (Lauretta et al., 1999, 2001; Meier et al., 2016). Lauretta et al. (2001) studied the Murchison and Allende carbonaceous chondrites and suggested that the

relative abundances of Hg isotopes in both meteorites are identical to terrestrial δ^{202}Hg values within 0.20‰–0.50‰. Conversely, Meier et al. (2016) showed that most carbonaceous chondrites exhibit slight MIF of the odd-numbered isotopes ^{199}Hg and ^{201}Hg ($\sim$–0.1‰ < Δ^{199}Hg < $\sim$0.4‰; $\sim$–0.18‰ < Δ^{201}Hg < $\sim$0.23‰), while noncarbonaceous chondrites and most achondrites show no MIF. Distinctively, all meteorites studied by Meier et al. (2016) showed isotopically light Hg (δ^{202}Hg = –7‰ to –1‰) relative to Earth's average crustal values, suggesting that Earth has lost a significant fraction of its primordial Hg during planetary differentiation or during late accretion of chondritic materials to Earth (Moynier et al., 2020), resulting in different Hg isotope signatures between the surface and deep-Earth reservoirs. At Bidart, δ^{202}Hg values in the Danian sediments above 50 cm contrast with the Hg isotopic composition of the Maastrichtian–lower Danian interval (Fig. 2), showing a large shift to negative values typical of carbonaceous chondrites, possibly representing remobilized impactor Hg that was redeposited on the seafloor. Thus, while our data may show an Hg isotope signature of the impactor, the very low Hg concentrations indicate it could not be the source of the Hg enrichments observed below the impact level. The high Δ^{199}Hg, Δ^{201}Hg, and δ^{202}Hg values observed above the boundary may also represent a period of increased photoreduction during the time when there was strong Hg mobilization from biomass burning, volcanic eruptions, and impactor input. The slightly but significantly different isotopic compositions in Δ^{199}Hg and Δ^{201}Hg within the 50 cm above the boundary and $\sim$100 cm below the boundary virtually exclude the interpretation that the Hg found in the lower part was simply mixed down from the boundary level.

CONCLUSIONS

The results of our study reveal that Deccan Traps eruptions led to enhanced Hg deposition prior to and during the Chicxulub asteroid impact, and continued into the earliest Danian. This period of intense volcanism is consistent with recent high-precision U-Pb ages that place the largest eruptions of the Deccan Traps prior to or straddling the K-Pg boundary (Schoene et al., 2019). Deccan Traps volcanism clearly had a global effect, and whether the Chicxulub impact was the proverbial "straw that broke the camels back", or was an inconsequential random event that occurred during an ongoing extinction, remains to be elucidated.

ACKNOWLEDGMENTS

This work was funded by Natural Science Foundation of 225 China (grants 41625012, 41961144028, 41830647) (J. Chen) and the Fundação para a Ciência e Tecnologia / UIDB/50019/2020–IDL (E. Font). We thank Stephen Grasby, Matthias Meier, and Hamed Sanei for their help in improving the quality of the manuscript.

REFERENCES CITED

Alvarez, L.W., Alvarez, W., Asaro, F., and Michel, H.V., 1980, Extraterrestrial cause for the Cretaceous-Tertiary extinction—Experimental results and theoretical interpretation: Science, v. 208, p. 1095–1108, https://doi.org/10.1126/science.208.4448.1095.

Bergquist, B.A., and Blum, J.D., 2007, Mass-dependent and -independent fractionation of Hg isotopes by photoreduction in aquatic systems: Science, v. 318, p. 417–420, https://doi.org/10.1126/science.1148050.

Bergquist, R.A., and Blum, J.D., 2009, The odds and evens of mercury isotopes: Applications of mass-dependent and mass-independent isotope fractionation: Elements, v. 5, p. 353–357, https://doi.org/10.2113/gselements.5.6.353.

Blum, J.D., Sherman, L.S., and Johnson, M.W., 2014, Mercury isotopes in earth and environmental sciences: Annual Review of Earth and Planetary Sciences, v. 42, p. 249–269, https://doi.org/10.1146/annurev-earth-050212-124107.

Bonté, P., Delacotte, O., Renard, M., Laj, C., Boclet, D., Jehanno, C., and Rocchia, R., 1984, An iridium rich layer at the Cretaceous-Tertiary boundary in the Bidart section (southern France): Geophysical Research Letters, v. 11, p. 473–476, https://doi.org/10.1029/GL011i005p00473.

Colodner, D.C., Boyle, E.A., Edmond, J.M., and Thomson, J., 1992, Postdepositional mobility of platinum, iridium and rhenium in marine sediments: Nature, v. 358, p. 402–404, https://doi.org/10.1038/358402a0.

Courtillot, V., Besse, J., Vandamme, D., Montigny, R., Jaeger, J.J., and Cappetta, H., 1986, Deccan flood basalts at the Cretaceous-Tertiary boundary: Earth and Planetary Science Letters, v. 80, p. 361–374, https://doi.org/10.1016/0012-821X(86)90118-4.

Evans, N.J., and Chai, C.F., 1997, The distribution and geochemistry of platinum-group elements as event markers in the Phanerozoic: Palaeogeography, Palaeoclimatology, Palaeoecology, v. 132, p. 373–390, https://doi.org/10.1016/S0031-0182(97)00059-X.

Feyte, S., Gobeil, C., Tessier, A., and Cossa, D., 2012, Mercury dynamics in lake sediments: Geochimica et Cosmochimica Acta, v. 82, p. 92–112, https://doi.org/10.1016/j.gca.2011.02.007.

Font, E., and Bond, D., 2021, Volcanism and mass extinction, *in* Alderton, D., and Elias, S.A., eds., Encyclopedia of Geology, Volume 5 (2nd edition): London, Academic Press, p. 596–606.

Font, E., Nedelec, A., Ellwood, B.B., Mirao, J., and Silva, P.F., 2011, A new sedimentary benchmark for the Deccan Traps volcanism?: Geophysical Research Letters, v. 38, L24309, https://doi.org/10.1029/2011GL049824.

Font, E., Adatte, T., Sial, A.N., Drude de Lacerda, L., Keller, G., and Punekar, J., 2016, Mercury anomaly, Deccan volcanism, and the end-Cretaceous mass extinction: Geology, v. 44, p. 171–174, https://doi.org/10.1130/G37451.1.

Gobeil, C., Macdonald, R.W., and Smith, J.N., 1999, Mercury profiles in sediments of the Arctic Ocean basins: Environmental Science & Technology, v. 33, p. 4194–4198, https://doi.org/10.1021/es990471p.

Grasby, S.E., Them, T.R., Chen, Z.H., Yin, R.S., and Ardakani, O.H., 2019, Mercury as a proxy for volcanic emissions in the geologic record: Earth-Science Reviews, v. 196, 102880, https://doi.org/10.1016/j.earscirev.2019.102880.

Huang, Q., Liu, Y.L., Chen, J.B., Feng, X.B., Huang, W.L., Yuan, S.L., Cai, H.M., and Fu, X.W., 2015, An improved dual-stage protocol to pre-concentrate mercury from airborne particles for precise isotopic measurement: Journal of Analytical Atomic Spectrometry, v. 30, p. 957–966, https://doi.org/10.1039/C4JA00438H.

Keller, G., Mateo, P., Punekar, J., Khozyem, H., Gertsch, B., Spangenberg, J., Bitchong, A.M., and Adatte, T., 2018, Environmental changes during the Cretaceous-Paleogene mass extinction and Paleocene-Eocene thermal maximum: Implications for the Anthropocene: Gondwana Research, v. 56, p. 69–89, https://doi.org/10.1016/j.gr.2017.12.002.

Keller, G., et al., 2020, Mercury linked to Deccan Traps volcanism, climate change and the end-Cretaceous mass extinction: Global and Planetary Change, v. 194, 103312, https://doi.org/10.1016/j.gloplacha.2020.103312.

Lauretta, D.S., Devouard, B., and Buseck, P.R., 1999, The cosmochemical behavior of mercury: Earth and Planetary Science Letters, v. 171, p. 35–47, https://doi.org/10.1016/S0012-821X(99)00129-6.

Lauretta, D.S., Klaue, B., Blum, J.D., and Buseck, P.R., 2001, Mercury abundances and isotopic compositions in the Murchison (CM) and Allende (CV) carbonaceous chondrites: Geochimica et Cosmochimica Acta, v. 65, p. 2807–2818, https://doi.org/10.1016/S0016-7037(01)00630-5.

Martin-Peinado, F.J., and Rodriguez-Tovar, F.J., 2010, Mobility of iridium in terrestrial environments: Implications for the interpretation of impact-related mass extinctions: Geochimica et Cosmochimica Acta, v. 74, p. 4531–4542, https://doi.org/10.1016/j.gca.2010.05.009.

Meier, M.M.M., Cloquet, C., and Marty, B., 2016, Mercury (Hg) in meteorites: Variations in abundance, thermal release profile, mass-dependent and mass-independent isotopic fractionation: Geochimica et Cosmochimica Acta, v. 182, p. 55–72, https://doi.org/10.1016/j.gca.2016.03.007.

Meyer, K.W., Petersen, S.V., Lohmann, K.C., Blum, J.D., Washburn, S.J., Johnson, M.W., Gleason, J.D., Kurz, A.Y., and Winkelstern, I.Z., 2019, Biogenic carbonate mercury and marine temperature records reveal global influence of Late Cretaceous Deccan Traps: Nature Communications, v. 10, 5356, https://doi.org/10.1038/s41467-019-13366-0.

Moynier, F., Chen, J.B., Zhang, K., Cai, H.M., Wang, Z.C., Jackson, M.G., and Day, J.M., 2020, Chondritic mercury isotopic composition of Earth and evidence for evaporative equilibrium degassing during the formation of eucrites: Earth and Planetary Science Letters, v. 551, 116544, https://doi.org/10.1016/j.epsl.2020.116544.

Percival, J.B., and Outridge, P.M., 2013, A test of the stability of Cd, Cu, Hg, Pb and Zn profiles over two decades in lake sediments near the Flin Flon smelter, Manitoba, Canada: The Science of the Total Environment, v. 454, p. 307–318, https://doi.org/10.1016/j.scitotenv.2013.03.011.

Pospichal, J.J., Wise, J.S.W., Asaro, F., and Hamilton, N., 1990, The effects of bioturbation across a biostratigraphically complete high southern latitude Cretaceous/Tertiary boundary, *in* Sharpton, V.L., and Ward, P.D., eds., Global Catastrophes in Earth History: An Interdisciplinary Conference on Impacts, Volcanism, and Mass Mortality: Geological Society of America Special Paper 247, p. 497–508, https://doi.org/10.1130/SPE247-p497.

Preisinger, A., Zobetz, E., Gratz, A.J., Lahodynsky, R., Becke, M., Mauritsch, H.J., Eder, G., Grass, F., Rogl, F., Stradner, H., and Surenian, R., 1986,

The Cretaceous-Tertiary boundary in the Gosau Basin, Austria: Nature, v. 322, p. 794–799, https://doi.org/10.1038/322794a0.

Schoene, B., Eddy, M.P., Samperton, K.M., Brehin Keller, C., Keller, G., Adatte, T., and Khadri, S.F.R., 2019, U-Pb constraints on pulsed eruption of the Deccan Traps across the end-Cretaceous mass extinction: Science, v. 363, p. 862–866, https://doi.org/10.1126/science.aau2422.

Schulte, P., et al., 2010, The Chicxulub asteroid impact and mass extinction at the Cretaceous-Paleogene boundary: Science, v. 327, p. 1214–1218, https://doi.org/10.1126/science.1177265.

Sial, A.N., Lacerda, L.D., Ferreira, V.P., Frei, R., Marquillas, R.A., Barbosa, J.A., Gaucher, C., Windmoller, C.C., and Pereira, N.S., 2013, Mercury as a proxy for volcanic activity during extreme environmental turnover: The Cretaceous-Paleogene transition: Palaeogeography, Palaeoclimatology, Palaeoecology, v. 387, p. 153–164, https://doi.org/10.1016/j.palaeo.2013.07.019.

Sial, A.N., Chen, J.B., Lacerda, L.D., Peralta, S., Gaucher, C., Frei, R., Cirilli, S., Ferreira, V.P., Marquillas, R.A., Barbosa, J.A., Pereira, N.S., and Belmino, I.K.C., 2014, High-resolution Hg chemostratigraphy: A contribution to the distinction of chemical fingerprints of the Deccan volcanism and Cretaceous-Paleogene boundary impact event: Palaeogeography, Palaeoclimatology, Palaeoecology, v. 414, p. 98–115, https://doi.org/10.1016/j.palaeo.2014.08.013.

Sial, A.N., Chen, J.B., Lacerda, L.D., Frei, R., Tewari, V.C., Pandit, M.K., Gaucher, C., Ferreira, V.P., Cirilli, S., Peralta, S., Korte, C., Barbosa, J.A., and Pereira, N.S., 2016, Mercury enrichment and Hg isotopes in Cretaceous-Paleogene boundary successions: Links to volcanism and palaeoenvironmental impacts: Cretaceous Research, v. 66, p. 60–81, https://doi.org/10.1016/j.cretres.2016.05.006.

Smit, J., Koeberl, C., Claeys, P., and Montanari, A., 2016, Mercury anomaly, Deccan volcanism, and the end-Cretaceous mass extinction: Comment: Geology, v. 44, p. e381, https://doi.org/10.1130/G37683C.1.

Sprain, C.J., Renne, P.R., Vanderkluysen, L., Pande, K., Self, S., and Mittal, T., 2019, The eruptive tempo of Deccan volcanism in relation to the Cretaceous-Paleogene boundary: Science, v. 363, p. 866–870, https://doi.org/10.1126/science.aav1446.

Zambardi, T., Sonke, J.E., Toutain, J.P., Sortino, F., and Shinohara, H., 2009, Mercury emissions and stable isotopic compositions at Vulcano Island (Italy): Earth and Planetary Science Letters, v. 277, p. 236–243, https://doi.org/10.1016/j.epsl.2008.10.023.

Zhou, L., Kyte, F.T., and Bohor, B.F., 1991, Cretaceous-Tertiary boundary of DSDP Site 596, South Pacific: Geology, v. 19, p. 694–697, https://doi.org/10.1130/0091-7613(1991)019<0694:CTBODS>2.3.CO;2.

Printed in USA